Topographic Effects on the Texture of High-Resolution Forest-Stand Images Measured by the Semivariogram

Benoît St-Onge

Abstract

By studying the statistical relationship between terrain gradient and the range of the semivariogram of simulated high-resolution images of forest stands, we assessed the effects of topography on estimates of tree size and density obtained through texture measures. Three-dimensional computer models of hardwood and softwood forest stands were overlaid on slopes of varying gradient. Using a geometrical-optical approach, one-meter-resolution images were generated in 120 series representing different combinations of forest types and sun-terrain geometry. The range of the semivariogram of these images was measured in four directions and its relation with gradient was evaluated through regression. Results show that topography affects texture mostly in sparse stands, and that the gradient-induced absolute error in the estimates of tree size and density is low.

Introduction

Visual texture analysis, which has traditionally been recognized as an important part of the process of interpreting large-scale photographs of the forest (Küchler, 1967; Howard, 1970), can be automated and included in forest mapping procedures based on image processing. Many texture features, such as coarseness, anisotropy, linearity, etc., have indeed been adequately measured by classical computer algorithms (Tamura *et al.*, 1978; Haralick, 1979; Levine, 1985). The application of these algorithms to the task of forest mapping is however experimental, and some problems remain to be solved before an automated mapping method based at least in part on automated texture analysis, such as the one we have proposed in earlier studies (St-Onge and Cavayas, 1995; St-Onge and Cavayas, 1997), can be made operational. One of these problems lies in the distortion of image texture caused by topography. Indeed, the two-dimensional arrangement of tree shadows, which constitute the main source of texture on high-resolution images, is controlled by the three-dimensional structure of forest stands. Because terrain gradient affects this structure through a change in inter-tree altitude relations, image texture can theoretically be altered in ways that could lead to errors in automated or visual estimation of tree size, stand density, crown closure, and the like.

Although it is generally recognized that topography affects the appearance of the forest on large-scale aerial photographs (Spurr, 1960; Avery and Burkhart, 1983), not much is known about the quantitative relationship between terrain gradient and forest image texture. While some parallel studies have shown the measurable influence of terrain gradient on the bidirectional reflectance distribution function (BRDF) of tree canopies (e.g., Barker Schaaf *et al.*, 1994), or on the propagation of solar radiation through forest canopies (Rowland and Moore, 1992), no systematic research concerning the effects of topography on image texture has, to our knowledge, been published. This situation probably arises from the fact that a great number of remote sensing research undertakings focus on forest mapping at a resolution (typically 30 m) where topography affects spectral signatures more than it alters the image spatial structure (e.g., Ekstrand, 1996). However, the advent of very-high-resolution satellite sensors, such as *QuickBird* and *Orbview* (Hamilton, 1996), will undoubtedly trigger the development of new texture-based mapping methods. In this context, the systematic study of the topography's influence on texture clearly gains importance. The general objective of our research effort was thus to show, in a quantitative fashion, the influence of terrain gradient on the texture of one-meter computer simulated panchromatic images of the forest generated from three-dimensional models of trees overlaid on a slope. We studied this relationship, on a stand basis, for eight different types of forest canopies and for 15 different sun-terrain configurations by varying the sun elevation and azimuth. Our goal was also to assess the feasibility of rectifying topography-altered texture estimates by applying correction equations developed from an empirical knowledge of the mathematical relationships between gradient and texture, and by using a digital elevation model.

In the following sections, we briefly review progress in forest mapping involving texture analysis and introduce a texture measure based on the directional semivariogram. We then describe the geometrical-optical method used to generate three-dimensional computer representations of forest stands on sloping terrain, as well as the method used to generate the computer simulated images. A presentation of the experimental procedure employed to reveal the influence of topography on image texture follows. Finally, we show the details of the experimental results for the different types of forest stands and discuss the factors affecting the relationship between terrain gradient and image texture.

Forest Mapping Using Texture Analysis

Texture is generally defined as being the result of the systematic or random repetition of some elementary patterns over an area that is large in comparison to the pattern sizes (Hawkins, 1970; Haralick, 1979), i.e., spatially structured gray-level variations at a relatively high spatial frequency.

GEIGER, Department of Geography, University of Québec in Montréal, Case postale 8888, Montréal, Québec H3C 3PB, Canada (st-onge.benoit@uqam.ca).

Photogrammetric Engineering & Remote Sensing, Vol. 65, No. 8, August 1999, pp. 923–935.

0099-1112/99/6508–923$3.00/0

This phenomenon is observed on most types of forest images, from high resolution aerial photographs to coarser images taken from various orbital platforms. It has been demonstrated that the horizontal and vertical structure of forest canopies determine image texture in ways that vary according to their spatial resolution (Küchler, 1967). In high-resolution images, the light and dark patterns created by sun-lit crowns and projected shadows become the dominant factor that determines image texture (Howard, 1970). These patterns are typically observed on medium-scale photographs (approximately 1:15,000) employed in forest-stand mapping, or on aerial digital images having a resolution between 0.5 and 4 m (St-Onge *et al.*, 1991). The size, shape, an stocking of trees, and, more generally, the three-dimensional structure of the canopy (Howard, 1970), determine shadow patterns, thus allowing the assessment of canopy structure through image texture analysis.

A wide range of computer algorithms exist that are able to automatically derive image-texture attributes by measuring certain statistical features of the image function. Most common texture measures are based on the co-occurrence matrix (Haralick, 1986), the Fourier spectrum (Stromberg and Farr, 1986), auto-regressive models (Kashyap, 1986), the semivariogram (Woodcock *et al.*, 1988; Franklin *et al.*, 1992), etc. More recent approaches include wavelet analysis (Unser, 1995) and implementation using neural networks (Dreyer, 1993). Numerous studies have employed some type of texture measure to map forest canopies. The usual approach consists in applying a multispectral per-pixel classification to spectral channels combined to texture channels generated by an automated analysis (Teillet *et al.*, 1981; Dikshit and Roy, 1992). While this approach was shown to improve spectral classifications of images having a resolution between one and 30 m, the gain in effectiveness were usually marginal, the increase in the percentage of correctly classified pixels being in most cases less than 10 percent (Dikshit, 1996). Because texture contents increases with resolution (Marceau *et al.*, 1990; Wang and He, 1990), more encouraging results were obtained for images having a resolution of a few meters or less (Gougeon and Wong, 1987; Vlcek *et al.*, 1987; Atkinson and Danson, 1988; Woodcock *et al.*, 1988; Cohen *et al.*, 1990; St-Onge and Cavayas, 1995), in which case texture information was often exploited directly, i.e., without recourse to a mixed classification involving spectral information. However, no attempt was made in these research efforts to tackle the issue of topography.

In this study, texture analysis was conducted using the range of the semivariogram. Stemming from the field of geostatistics (Matheron, 1970), the semivariogram (γ) measures the average gray-level difference between pixels (x and $x + h$) separated by lag h: i.e.,

$$2\gamma(h) = \mathrm{E}[f(x + h) - f(x)]^2. \quad (1)$$

In many remote sensing images, this difference is low at short lags because of the high autocorrelation between neighboring pixels. As the lag increases, the average difference climbs and tends to level off past a certain inter-pixel distance, revealing the fact that, after a given range, there exists no correlation between two pixels; therefore, augmenting the lag does not increase the average gray-level difference. The range is often proportional to the texture coarseness and its directional variation reflects the anisotropy of the texture, an indicator of the linearity and "orientedness" of the elementary image patterns.

Our ongoing work on texture analysis aims at relating forest structure parameters, such as crown diameter, number of trees per hectare, etc., to the directional semivariogram ranges by way of multiple-regression equations (St-Onge and Cavayas, 1995; St-Onge and Cavayas, 1997). The ranges are first estimated by fitting a theoretical model to the experimental semivariograms computed for forest-stand training images of known crown diameter, density, and percent cover. A multiple-regression analysis is then conducted in order to build a prediction equation for each forest parameter based on the training set statistics. The resulting equations can then be applied to forest images to obtain estimates of stand structure, and also serve as a basis for automated segmentation of forest images. We present two such equations taken from St-Onge and Cavayas (1995) to give an overview of their structure. We will refer to them later to demonstrate how range distortions caused by topography translate into absolute error in the estimates of crown diameter (CD) and stand density (SD): i.e.,

$$\mathrm{CD} = 0.62 - 0.50\, a_{\mathrm{par}} + 1.53 a_{\mathrm{per}} + 0.33\, |a_{\mathrm{par}} - a_{\mathrm{per}}| \quad (2)$$

$$\ln \mathrm{SD} = 8.04 - 0.20\, a_{\mathrm{par}} + 0.02\, a_{\mathrm{per}} + 0.15 \ln |a_{\mathrm{par}} - a_{\mathrm{per}}| - 1.45 \ln a_{\mathrm{mid}} \quad (3)$$

where a_{par}, a_{per}, and a_{mid} are the semivariogram ranges calculated respectively in the directions parallel to the sun's azimuth, perpendicular to the sun's azimuth, and in medial direction (45 degrees from both parallel and perpendicular directions). These equations were developed from a training set composed of computer-simulated images of various types of softwood stands. The estimates obtained through these equations are typically within 20 percent of the actual values (St-Onge and Cavayas, 1997). The resulting forest maps obtained by applying a region-growing algorithm to the estimates bear a high level of detail, showing homogeneous forest patches as small as one hectare.

Data and Models

Studying the slope-texture relationships for a wide variety of forest and illumination conditions demands a complex apparatus if done by using real images and ground-truth measures. Indeed, comparable forest stands for different slope and aspect situations must be found, measured, imaged, and georeferenced. Minute differences, such as gap size, between basically comparable stands, i.e., stands of similar height and density, or variations in sun elevation, can create significant semivariance discrepancies that would mask the effects of topography. In these conditions, it is unlikely that a sufficient number of images and ground data could be acquired and used to generate valid statistical results, in a reasonable amount of time. We have therefore chosen to use geometrical three-dimensional representations of forest stands placed on planes of varying gradient as a means to generate computer-simulated images that allow the study of topographical effects to be made in controlled conditions. This approach has been utilized in a variety of purposes pertaining to bidirectional reflectance distribution function or spatial structure modeling (Li and Strahler, 1985; Ryherd and Woodcock, 1996). We demonstrate the degree of textural resemblance between simulated and real images later in this section.

In this study, we aimed at producing one-meter-resolution panchromatic images that imitate some of the characteristics of the images that will be acquired from the new orbital platforms equipped with very-high-resolution sensors (*Space Imaging*, Orbimage's *Orbview*, and Earthwatch's *QuickBird*; Hamilton, 1996) with a spatial resolution comparable to that of medium-scale aerial photographs, a high geometric accuracy ensured by a stable platform, and minimal tree leaning associated with the near vertical viewing angles resulting from the narrow swath width.

In our modeling approach, individual trees form the basic elements of the three-dimensional representation of each stand. In the current study, hardwoods were modeled as an ellipsoid on a stick (as suggested by and McKelvey (1987)

and Koop (1989)) and softwood were given a bullet shape that resembles that of most spruce trees: a cone-like profile at the top of the tree changing gradually to a cylinder profile going down, as suggested by Stiell (1962), and using the implementation presented in our earlier work (St-Onge and Cavayas, 1995). The shape of the trees is also defined by the crown ratio (the percentage of total tree height occupied by the live crown) and the width ratio (the ratio of maximum crown radius to live crown length). To simplify the modeling process, these proportions were kept invariable for each class of tree models but were calibrated by *in situ* measures made on live trees of the mixed forest of meridional Quebec, Canada. Each three-dimensional tree was generated by calculating the tree envelope from its total height and proportions, and the actual "planting" was done by updating each pixel of a two-layer one-meter-resolution grid with the minimum and maximum height values of the vertically projected tree model. We consider this modeling strategy better suited than simpler 2.5D schemes (a single layer matrix where the crown must occupy the full length of the tree, as in Ryherd and Woodcock (1996)) and more efficient than computer-intensive full-vector representations, because 8400 different tree stands were generated for this study.

The tree-size frequency distribution in a stand was generated using a Weibull distribution with a shape factor of 8.0 ($\beta = 8.0$) and a dispersion factor of 15.0 ($\chi = 15.0$). The Weibull distribution was chosen because of its wide acceptance in the literature as a good function to model tree-size class frequencies (Hafley and Schreuder, 1977; Minor *et al.*, 1985). The values for parameters β and χ were given to reproduce an uneven-aged structure where the co-dominants constitute the single class with the highest frequency, the dominants, intermediate, and suppressed trees being fewer. Very small trees were not included in the stand models because they cannot be resolved in one-meter images and because they are in most cases hidden by taller and wider trees. Tree locations were determined by using a random coordinate generator and by maintaining a minimum distance of 0.5 m between any two tree stems.

The gradient of the terrain was created by linearly increasing the virtual ground elevation from the left to the right of each image. After tree plantation, the three-dimensional terrain-stand models were illuminated by parallel rays simulating those of the sun. The brightness of each component (tree, understory vegetation) of the image was determined by its nominal reflectance and the Lambertian model. Shadows were created by projecting the tree envelopes on the ground and other tree crowns. A full description of the image synthesis procedure used here can be found in St-Onge and Cavayas (1995).

Because validation using real images is made difficult by the experimental structure, we compared real images with their computer-simulated equivalent. Twenty plots measuring approximately 20 by 20 meters were imaged by the MEIS II pushbroom scanner (Till *et al.*, 1987) at an altitude of 730 m, yielding a resolution of 36 cm in eight spectral bands. Tree position, species, height, and crown diameter were measured for each tree of those plots. These data, in conjunction with geometrical tree models having the appropriate shape, were used to generate computer images of the same resolution for the red spectral band. The following preprocessing steps were applied to render the images comparable: (1) geometric correction of the MEIS II sub-images representing the plots using bilinear resampling, and (2) low-pass filtering of the simulated images using a 3- by 3-pixel average filter to emulate the effect of the bilinear resampling and the histogram equalization of both real and simulated images to make their first-order statistics comparable. The semivariances were then evaluated in four different directions for each set of images, and the degree of concordance was assessed by visually comparing the variograms. Results for one plot are shown in Figure 1. They indicate that, even if some differences are observable in the images, the variograms agree very closely, mostly because the patterns of lit and shadowed canopy parts are very similar. This similarity suggests that the study of texture-gradient relationships based on simulated images would yield appropriate conclusion.

Evaluating the Effect of Slope on Texture

The interaction between the incident light and a forested surface can theoretically result in a very complex reflectance behavior when the position of the sun relative to the slope changes. This fact has been demonstrated for the BRDF (Barker Schaaf *et al.*, 1994). Because we suspected that the spatial structure changes of the image caused by varying sun-terrain geometries would exhibit a behavior at least as complex as that of the BRDF, and because many different such geometries had to be evaluated in order to establish the relationship between terrain gradient and image texture for given forest-stand structures, we divided the experiments into different classes of configurations. Thus, for each forest type, sun elevation relative to the horizon (θ_s) was varied from 40 to 60 degrees with ten-degree intervals (three increments) and the angular difference between sun and gradient azimuths (φ_{sg}) took values from 0 degrees to 180 degrees with 45-degree intervals (five increments). Our intent was also to examine the gradient-texture variations for a certain number of stand types: young open forest, young dense forest, mature open forest, and mature dense forest, for both softwoods and hardwoods. Thus, eight different types of stands were generated from a combination of two types of trees, two different average tree heights (10 m and 25 m, having crown diameters of 2 and 5 m, respectively) and two different densities (500 and 1500 trees/ha). The resulting percent cover for the four combinations of height and densities were 15 percent, 40 percent, 64 percent, and 97 percent (Tables 1 and 2).

Each image series concerned a particular combination of forest type, sun azimuth, and sun elevation. Within each series, the terrain gradient was varied from 0 to 30 degrees using five-degree intervals (seven increments). To achieve a good level of statistical significance without overburdening the experimental process, ten images were generated for each of the seven slope increments, yielding 70 image series. On each image, the semivariogram was measured in four directions, which can be characterized either by their angular difference with the azimuth of the gradient, φ_{mg}, or by their angular difference with the azimuth of the sun, φ_{ms}. In every case, measures in the directions parallel ($\varphi_{ms} = 0°$) and perpendicular ($\varphi_{ms} = 90°$) to the azimuth of the light source, and measures parallel ($\varphi_{ms} = 0°$) and perpendicular ($\varphi_{mg} = 90°$) to the maximum gradient of the terrain were made. The two former directions normally correspond respectively to the maximum and minimum ranges in a high-resolution image of a forest stand. Indeed, they give an estimation of the anisotropy that results from the elongation of shadows in the direction away from the light source when percent cover is low. The latter two directions were considered due to the fact that they correspond respectively to the minimum and maximum variations in the three-dimensional structure of the stand due to varying gradient.

Results

The influence of terrain gradient on texture coarseness, as estimated by the range of the semivariogram, is reported here by means of graphs and regression statistics. Appraisal of the behavior of this influence was done in part by visual analysis of the plots of slope versus semivariogram ranges. However, because showing these slope-texture graphs for all of

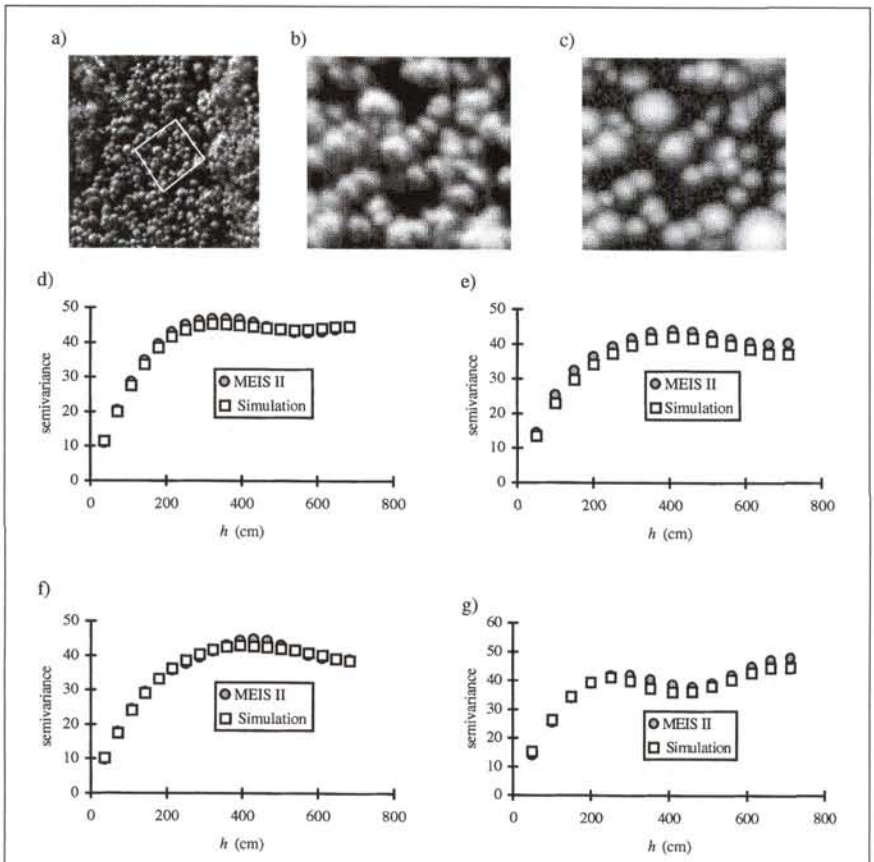

Figure 1. Comparison of the semivariance of a real MEIS II image (b) and equivalent computer simulated image (c) for a 20- by 20-meter plot (a) measured in four directions relative to the sun's azimuth: parallel (d), 45 degrees (e), perpendicular (f), and 135 degrees (g).

the 120 combinations of forest and illumination parameters was impossible within the scope of this paper, only the most significant curves are shown. For the same reason, the coefficient of determination (R^2) and the slope of the mathematical relationship (b) between gradient and the range of the semivariogram, obtained through simple linear regression of the latter two variables, are also provided in order to summarize the strength of the relationship for each situation (Tables 1 and 2), and were used as an additional means to evaluate the results. Regression and statistical significance were evaluated using the SPSS software package. Finally, a sample of computer-simulated stand images is shown in Figure 2 to exemplify the visual effect of varying terrain gradient in different sun-terrain geometries. We first present general results and a comparison of hardwoods and softwoods because they will help simplify further accounts of topography-texture relationships.

The influence of topography is most often weak, even nil, but can in particular situations be relatively strong, as is the case, for example, of a 500-trees/ha stand composed of 10-m trees (Figure 3). R^2 and b values reach a maximum of 0.95 and 0.09, respectively, which indicates that, in some cases, the range of the semivariogram nearly doubles when the terrain gradient is increased from 0 to 30 degrees (Figure 3). When the influence appears, it is often measurable over the entire range of the gradient variation, even for low gradients (from 0 to 5 degrees). From Equations 2 and 3, and using the data appearing in Figure 3 (trees having a crown diameter of 2 m and a density of 500 trees/ha), we can deduce that, in this particular case, the increase of the range in the direction parallel to the light source azimuth would bring about errors of approximately 60 cm in the estimation of crown diameter (1.5 m instead of 2.1 m, using $a_{par} = 4.0$ at 0 degrees and $a_{par} = 7.8$ at 30 degrees, and $a_{per} = 1.8$), and a 220-trees-per-hectare difference in density (265 instead of 485 trees/ha, using the same values for a_{par} and a_{per}, and $a_{mid} = 2.3$). For both quantities, the relative error is quite high; however, in the context of a remote sensing inventory of the forest, the absolute error can be qualified as being rather small. Because the magnitude of the error is far less for higher densities (1500 trees/ha) or size (crown diameter of 5 m), as it will be demonstrated in the following lines, it appears that the absolute error in the estimation of certain stand structure parameters remains quite low, even in the most extreme cases.

The shape of the tree crowns is the main factor responsible for differences in the three-dimensional structures of hardwood and softwood stands. The conical or bullet shape of softwood crowns will let more light reach the lower parts of the canopy on the sunlit side of trees and will allow for longer shadows because of the openness of the top part of the canopy. It was suspected that a difference in crown shape would yield a difference in (1) the average variogram values and in (2) the topography-texture relation. The results shown in Tables 1 and 2, however, indicate that, while the former hypothesis was found to be true, the latter is generally false. Indeed, significant relationships are in most cases observed for the same combinations of tree size, stand den-

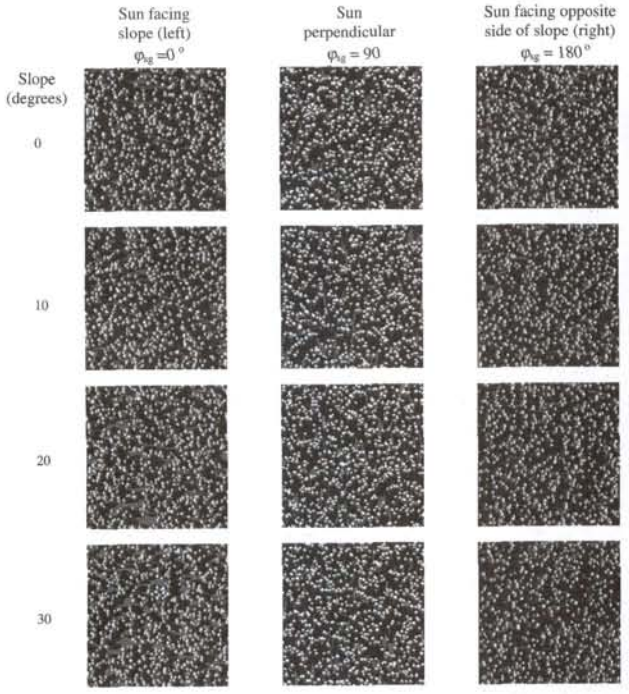

Figure 2. Example of the effect of terrain gradient on image texture for three different light source directions (20-m softwood trees with a density of 500 trees/ha).

sity, and sun position. Moreover, the shapes of the curves are approximately the same for both types of trees, even though magnitude may vary. One typical example of this similarity in the behavior of gradient influence appears in Figure 4 (stands with a very low crown closure lit at grazing angle). We first observe that the range estimates have a smaller variance and greater maximum values (at least for the ranges measured along the gradient) in the case of softwood trees. The evolution of the curve is nonetheless similar: a rise culminating at gradients of 10 or 15 degrees, followed by an almost equivalent drop. Note that this kind of behavior is rather rare and, despite the clear influence of the gradient, is not reflected in the regression coefficients due to the non monotonic quality of the relation. Some minor behavior differences were observed, mainly for stands with a very low crown closure. Figure 5 exemplifies these occasional dissimilarities. It is easy to see that the well defined drop in the softwood stand ranges is almost unnoticeable for the hardwoods. The occurrences of divergence between softwood and hardwood curve behavior are so few that we are lead to conclude that only minor differences exist between the effect of slope on the ranges measured over softwood and hardwood stand images. Some differences are also visible in Tables 1 and 2, but we can observe that the minima and maxima in the strength of the topography-texture relationship occur for approximately the same forest and sun-slope geometry situations. The overall similarity suggests that three-dimensional protuberances will have roughly the same effect on texture-gradient relationships, even if the shape of those protuberances varies to a certain extent. It is also true that the geometrical shapes used to model trees, i.e., ellipsoids for hardwoods and a bullet shape for softwoods, are more similar than, say, a sphere (isolated oak) and a cylinder (black spruce growing at high latitudes), in which case stronger differences could be expected. Therefore, all further results will be presented without reference to one or the other type of tree.

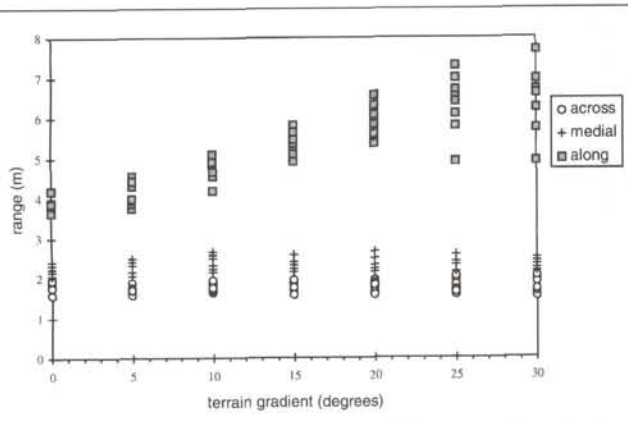

Figure 3. Case showing the strong influence of terrain gradient when percent cover is low (10-m trees with a density of 500 trees/ha).

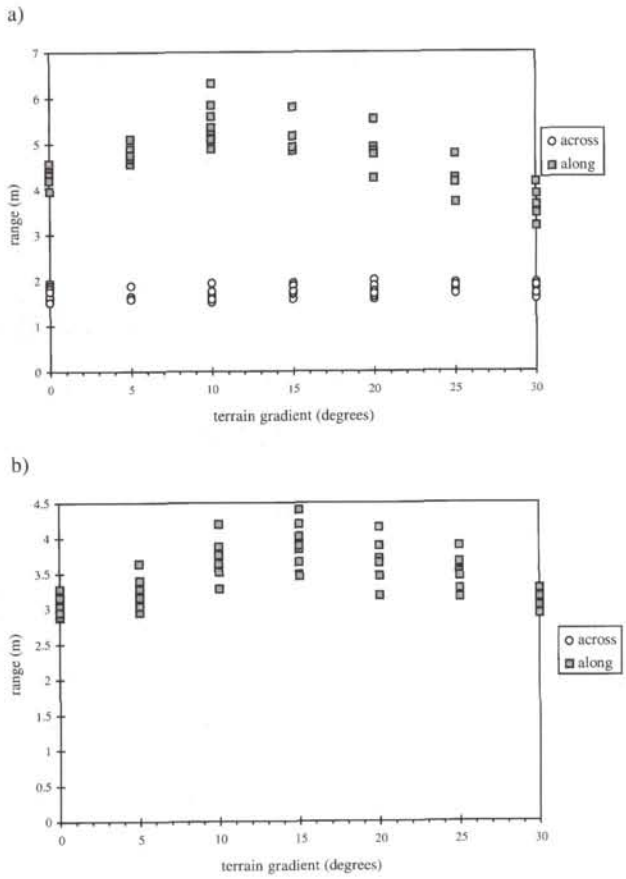

Figure 4. Comparison of the effect of terrain gradient on the range measured along (φ_{mg} = 0°) and across (φ_{mg} = 90°) the slope for softwoods (a) and hardwoods (b) at φ_{sg} = 90° and θ_s = 40° (10-m trees with a density of 500 trees/ha).

Tree size and stand density together produce the most sensible effect on the slope-texture relationship. In light of the results, it is suspected that crown closure alone determines the effects of terrain gradient increase on the semivariogram range. We see from Tables 1 and 2 that almost all

TABLE 1. SLOPE (B) AND COEFFICIENT OF DETERMINATION (R^2) OF THE REGRESSION MODEL BETWEEN TERRAIN GRADIENT AND THE SEMIVARIOGRAM DIRECTIONAL RANGES FOR DIFFERENT TYPES OF SOFTWOOD STANDS, SUN ELEVATION, AND AZIMUTH.

$\varphi_{sg} = 0°$													
Stand density		500 trees/hectare						1500 trees/hectare					
Tree height		10 meters			25 meters			10 meters			25 meters		
Percent cover		15			40			64			97		
Sun elevation θ_s		40°	50°	60°	40°	50°	60°	40°	50°	60°	40°	50°	60°
$\varphi_{mg} = 0°$	R^2	.28465	.71566	.67469	.13685	.28095	.04078	.08387	.10216	.01077	.01245	.20095	.35226
($\varphi_{ms} = 0°$)	b	−.01411	−.02419	−.01596	5.61E-03	5.70E-03	2.64E-03	−4.24E-03	−4.41E-04	−8.57E-04	−4.00E-04	1.50E-03	3.58E-03
$\varphi_{mg} = 45°$	R^2	.06768	.13503	.00028	.07942	.01331	.01141	.00108	.04824	.15906	.00152	.03086	.00847
($\varphi_{ms} = 45°$)	b	4.11E-03	6.34E-03	−7.5E-04	−4.66E-03	2.35E-03	2.00E-03	2.21E-04	−1.46E-03	−2.32E-03	−5.71E-04	3.06E-03	1.60E-03
$\varphi_{mg} = 90°$	R^2	.00023	.01388	.0087	.1125	.03317	.13042	.10762	.01735	.22409	.11351	.00000	.00008
($\varphi_{ms} = 90°$)	b	2.14E-04	2.00E-03	−4.3E-03	−3.26E-03	−1.80E-03	−3.94E-03	−3.64E-03	−1.29E-03	−4.61E.-03	−3.43E-03	.00000	−8.57E-05
$\varphi_{mg} = 135°$	R^2	.06294	.06557	.13409	.01437	.00834	.01202	.08852	.02070	.00878	.02342	.00337	.00081
($\varphi_{ms} = 45°$)	b	3.84E-03	4.62E-03	−2.4E-03	−2.17E-03	1.78E-03	1.69E-03	−2.04E-03	1.02E-03	−7.71E-04	2.08E-03	9.14E-04	3.71E-04
$\varphi_{sg} = 45°$													
Stand density		500 trees/hectare						1500 trees/hectare					
Tree height		10 meters			25 meters			10 meters			25 meters		
Percent cover		15			40			64			97		
Sun elevation θ_s		40°	50°	60°	40°	50°	60°	40°	50°	60°	40°	50°	60°
$\varphi_{mg} = 0°$	R^2	.00048	.01765	.02553	.01216	.00025	.00708	.00255	.00635	.07827	.25958	.17433	.32737
($\varphi_{ms} = 45°$)	b	−5.42E-04	−2.9E-03	−3.35E-03	−1.03E-03	−1.71E-04	−7.71E-04	−1.92E-03	−4.84E-03	−0.1939	5.01E-03	4.32E-03	4.82E-03
$\varphi_{mg} = 45°$	R^2	.00127	.05583	.01248	.26189	.10530	.00985	.00008	.00013	.00681	.01227	.10844	.10215
($\varphi_{ms} = 0°$)	b	7.07E-04	4.42E-03	−1.64E-03	.13430	7.71E-03	1.6E-03	1.85E-04	1.57E-04	−1.11E-03	1.09E-03	4.24E-03	5.66E-03
$\varphi_{mg} = 90°$	R^2	.04727	.00308	.04181	.02507	.06520	.01426	.00188	.06936	.04059	.18632	.04624	.00241
($\varphi_{ms} = 45°$)	b	5.34E-03	−1.34E-03	−4.85E-03	−2.06E-03	−3.09E-03	−1.20E-03	−7.86E-04	−2.84E-03	−2.01E-03	−3.99E-03	−1.84E-03	−3.85E-04
$\varphi_{mg} = 135°$	R^2	.00079	.01573	.06240	.00027	.00081	.00275	.03655	.00198	.05597	.01315	.04457	.05228
($\varphi_{ms} = 90°$)	b	3.93E-04	−1.62E-03	−3.74E-03	−2.5E-04	−3.86E-04	−8.00E-04	−2.76E-03	−4.93E-04	−1.61E-03	3.77E-03	−6.14E-03	7.84E-03
$\sigma_{sg} = 90°$													
Stand density		500 trees/hectare						1500 trees/hectare					
Tree height		10 meters			25 meters			10 meters			25 meters		
Percent cover		15			40			64			97		
Sun elevation θ_s		40°	50°	60°	40°	50°	60°	40°	50°	60°	40°	50°	60°
$\varphi_{mg} = 0°$	R^2	.00047	.01464	.00130	.00199	.05839	.02024	.01438	.02560	.00323	.00485	.06905	.08682
($\varphi_{ms} = 90°$)	b	−2.14E-04	−1.09E-03	5.50E-04	5.14E-04	−2.31E-03	−1.71E-03	−1.14E-03	−1.35E-03	−3.64E-04	−7.86E-04	−3.07E-03	−2.60E-03
$\varphi_{mg} = 45°$	R^2	.11384	.17228	.06206	.00520	.00398	.00093	.00052	.09490	.03158	.02998	.03004	.00688
($\varphi_{ms} = 45°$)	b	3.37E-03	5.33E-03	3.69E-03	1.07E-03	1.16E-03	4.93E-04	−1.64E-04	2.06E-03	1.15E-03	2.39E-03	2.55E-03	1.32E-03
$\varphi_{mg} = 90°$	R^2	.88231	.66824	.46732	.03087	.01659	.01144	.04130	.10014	.00263	.02932	.00738	.00000
($\varphi_{ms} = 0°$)	b	.04801	.02700	.01108	1.54E-03	1.29E-03	9.43E-04	2.14E-03	3.41E-03	4.71E-04	5.14E-04	−3.14E-04	.00000
$\varphi_{mg} = 135°$	R^2	.22945	.30513	.01017	.02438	.10112	.01499	.00205	.04452	.03243	.00968	.07403	.02170
($\varphi_{ms} = 45°$)	b	6.33E-03	6.49E-03	1.41E-03	−2.75E-03	−4.92E-03	2.35E-03	−3.64E-04	−1.61E-03	−1.42E-03	−1.69E-03	−4.01E-03	−2.55E-03

TABLE 1 (CONT.)

$\varphi_{sg} = 135°$													
Stand density		500 trees/hectare						1500 trees/hectare					
Tree height		10 meters			25 meters			10 meters			25 meters		
Percent cover		15			40			64			97		
Sun elevation θ_s		40°	50°	60°	40°	50°	60°	40°	50°	60°	40°	50°	60°
$\varphi_{mg} = 0°$	R^2	.01903	.00278	.01960	.0265	.09132	.06257	.00872	.01661	.03130	.00319	.03775	.13063
($\varphi_{ms} = 45°$)	b	−3.58E-03	1.43E-03	−3.27E-03	5.14E-04	−3.43E-03	−2.23E-03	1.67E-03	−1.70E-03	−2.27E-03	−6.43E-04	−2.01E-03	−3.47E-03
$\varphi_{mg} = 45°$	R^2	.22641	.11231	.03632	.00000	.00038	.03783	.00760	.06597	.00101	.06386	.00061	.01531
($\varphi_{ms} = 90°$)	b	−7.79E-03	−5.41E-03	−2.66E-03	−7.14E-06	−3.21E-04	−2.27E-03	−1.29E-03	−3.01E-03	−2.14E-04	−6.65E-03	7.92E-04	−3.77E-03
$\varphi_{mg} = 90°$	R^2	.00787	.01439	.00872	.06305	.00029	.01704	.00522	.00920	.02154	.31808	.07632	.00516
($\varphi_{ms} = 45°$)	b	−2.34E-03	2.83E-03	−1.67E-03	2.91E-03	1.17E-04	−1.20E-03	1.27E-03	−1.13E-03	1.83E-03	6.34E-03	2.87E-03	6.43E-04
$\varphi_{mg} = 135°$	R^2	.01165	.38136	.65470	.10988	.00738	.02808	.02115	.24295	.18013	.02711	.01064	.06586
($\varphi_{ms} = 0°$)	b	6.64E-03	.07661	.05370	−1.54E-03	−1.54E-03	−2.91E-03	7.57E-03	.02999	.02810	−1.34E-03	−6.5E-04	−3.69E-03
$\varphi_{sg} = 180°$													
Stand density		500 trees/hectare						1500 trees/hectare					
Tree height		10 meters			25 meters			10 meters			25 meters		
Percent cover		15			40			64			97		
Sun elevation θ_s		40°	50°	60°	40°	50°	60°	40°	50°	60°	40°	50°	60°
$\varphi_{mg} = 0°$	R^2	.19660	.78002	.95066	.14467	.17145	.00353	.00759	.03897	.34670	.47549	.06347	.21735
($\varphi_{ms} = 0°$)	b	−.02934	.09437	.07161	4.35E-03	−3.82E-03	−6.43E-04	1.33E-03	−2.74E-03	.01140	6.12E-03	8.86E-04	−8.00E-04
$\varphi_{mg} = 45°$	R^2	.05163	.01283	.01019	.00400	.00005	.05555	.18471	.12926	.02116	.05034	.00684	.05250
($\varphi_{ms} = 45°$)	b	−3.47E-03	1.88E-03	−1.8E-03	1.06E-03	−1.21E-04	4.09E-03	5.28E-03	2.40E-03	1.10E-03	4.03E-03	1.33E-03	−3.40E-03
$\varphi_{mg} = 90°$	R^2	.03575	.00029	.00035	.03912	.05681	.07343	.29187	.19734	.08513	.10765	.09161	.03266
($\varphi_{ms} = 90°$)	b	2.27E-03	−2.00E-04	3.71E-04	2.06E-03	2.49E-03	2.57E-03	.01077	5.70E-03	2.91E-03	5.06E-03	−2.57E-03	−2.06E-03
$\varphi_{mg} = 135°$	R^2	.03440	.05620	.00116	.00873	.00816	.01307	.12106	.09343	.01632	.14658	.02864	.09677
($\varphi_{ms} = 45°$)	b	−2.89E-03	3.85E-03	5.71E-04	1.81E-03	−1.57E-03	1.89E-03	2.70E-03	2.16E-03	1.02E-03	7.14E-03	2.37E-03	−4.31E-03

TABLE 2. SLOPE (B) AND COEFFICIENT OF DETERMINATION (R^2) OF THE REGRESSION MODEL BETWEEN TERRAIN GRADIENT AND THE SEMIVARIOGRAM DIRECTIONAL RANGES FOR DIFFERENT TYPES OF HARDWOOD STANDS, SUN ELEVATION, AND AZIMUTH.

$\varphi_{sg} = 0°$												
Stand density		500 trees/hectare						1500 trees/hectare				
Tree height		10 meters			25 meters			10 meters			25 meters	
Percent cover		15			40			64			97	
Sun elevation θ_s		40°	50°	60°	40°	50°	60°	40°	50°	60°	40°	50°	60°
$\varphi_{mg} = 0°$	R^2	.00038	.21553	.63729	.40417	.43906	.35755	.00192	.00195	.02668	.00459	.43998	.67724
($\varphi_{ms} = 0°$)	b	−1.03E.-03	−5.25E-03	−8.06E-03	9.57E-03	.01369	.01436	2.57E-04	−2.57E-04	−6.43E-04	5.57E-04	6.30E.03	.01452
$\varphi_{mg} = 45°$	R^2	.00020	.05452	.04280	.07744	.07034	.11180	.01020	.03164	.07684	.04015	.01812	.21948
($\varphi_{ms} = 45°$)	b	−2.29E-04	−3.84E-03	−3.38E-03	5.37E-03	5.58E-03	6.92E-03	−1.18E-03	−2.49E-03	3.53E-03	−2.66E-03	2.16E-03	.01015
$\varphi_{mg} = 90°$	R^2	.01230	.00353	.08113	.00000	.00000	.03605	.19985	.09740	.11636	.12016	.16323	.33796
($\varphi_{ms} = 90°$)	b	−4.68E-03	−2.56E-03	−.01210	−1.43E-05	4.29E-05	−3.86E-03	−.01729	−.01280	−.01344	−7.16E-03	−9.07E-03	−.01359
$\varphi_{mg} = 135°$	R^2	.08387	.02364	.06868	.04220	.15487	.03586	.00474	.14409	.00262	.06762	.01990	.15988
($\varphi_{ms} = 45°$)	b	−5.17E-03	−2.83E-03	−3.93E-03	4.13E-03	8.84E-03	4.13E-03	9.71E-04	−5.42E-03	−6.71E-04	−3.24E-03	2.38E-03	7.93E-03
$\varphi_{sg} = 45°$												
Stand density		500 trees/hectare						1500 trees/hectare				
Tree height		10 meters			25 meters			10 meters			25 meters	
Percent cover		15			40			64			97	
Sun elevation θ_s		40°	50°	60°	40°	50°	60°	40°	50°	60°	40°	50°	60°
$\varphi_{mg} = 0°$	R^2	.16234	.15504	.20291	.33765	.21347	.19289	.03719	.02284	.00948	.34148	.48976	.53862
($\varphi_{ms} = 45°$)	b	−.01206	−.01026	−9.6E-03	.01299	9.09E-03	8.1E-03	−3.87E-03	3.26E-03	−2.34E-03	8.57E-03	.01183	.01654
$\varphi_{mg} = 45°$	R^2	.04811	.02113	.22364	.37285	.31292	.29806	.06208	.00712	.05411	.00138	.02515	.37388
($\varphi_{ms} = 0°$)	b	6.07E-03	−2.50E-03	−9.27E-03	9.16E-03	9.71E-03	.01117	2.64E-03	−9.57E-04	−2.04E-03	4.14E-04	1.61E-03	6.54E-03
$\varphi_{mg} = 90°$	R^2	.03066	.05750	.26893	.00008	.05193	.02954	.07212	.04794	.14538	.57807	.50460	.47523
($\varphi_{ms} = 45°$)	b	−5.31E-03	−6.09E-03	−.01326	1.29E-04	−3.90E-03	−3.04E-03	−4.23E-03	−4.19E-03	−9.03E-03	−.01055	−.01019	−8.08E-03
$\varphi_{mg} = 135°$	R^2	.02758	.03090	.00058	.04757	.01012	.00273	.02007	.03076	.00049	.30713	.16509	.37802
($\varphi_{ms} = 90°$)	b	−2.91E-03	−3.61E-03	−4.79E-04	−5.74E-03	−2.41E-03	−1.26E-03	2.39E-03	−3.13E-03	−3.07E-04	−.01731	−8.22E-03	−.01571
$\varphi_{sg} = 90°$												
Stand density		500 trees/hectare						1500 trees/hectare				
Tree height		10 meters			25 meters			10 meters			25 meters	
Percent cover		15			40			64			97	
Sun elevation θ_s		40°	50°	60°	40°	50°	60°	40°	50°	60°	40°	50°	60°
$\varphi_{mg} = 0°$	R^2	.0080	.02194	.06220	.07970	.09669	.03035	.02012	.00019	.09560	.30599	.39066	.25878
($\varphi_{ms} = 90°$)	b	−9.14E-04	−6.07E-03	−.01051	−5.64E-03	−6.11E-03	−3.63E-03	−5.56E-03	−5.64E-04	−.01216	−.01319	−.01626	−9.97E-03
$\varphi_{mg} = 45°$	R^2	.00937	.07093	.02089	.21249	.14653	.16817	.00002	.00243	.00002	.54259	.59489	.74955
($\varphi_{ms} = 45°$)	b	−1.71E-03	−4.41E-03	−2.2E-03	.01008	8.25E-03	7.77E-03	−7.86E-05	6.93E-04	−7.14E-05	.01754	.02103	.027444
$\varphi_{mg} = 90°$	R^2	.74264	.62700	.38160	.00086	.00192	.00378	.01808	.02741	.00306	.00163	.00725	.07480
($\varphi_{ms} = 0°$)	b	.03777	.02171	6.56E-03	3.43E-04	−4.57E-04	−8.43E-04	1.07E-03	1.11E-03	3.29E-04	2.57E-04	6E-04	2.1E-03
$\varphi_{mg} = 135°$	R^2	.00313	.00690	.02717	.27552	.31436	.30033	.00577	.01415	.00061	.71265	.66529	.49112
($\varphi_{ms} = 45°$)	b	1.01E-03	1.45E-03	2.71E-03	−8.27E-03	−8.74E-03	−.01044	−1.07E-03	−1.64E-03	−3.07E-04	−.01206	−.01129	−9.5E-03

TABLE 2 (CONT.)

$\varphi_{sg} = 135°$													
Stand density		500 trees/hectare						1500 trees/hectare					
Tree height		10 meters			25 meters			10 meters			25 meters		
Percent cover		15			40			64			97		
Sun elevation θ_s		40°	50°	60°	40°	50°	60°	40°	50°	60°	40°	50°	60°
$\varphi_{mg} = 0°$	R^2	.03110	.05240	.01462	.16012	.39783	.50050	.03941	.00007	.05534	.30984	.26369	.64664
($\varphi_{ms} = 45°$)	b	−5.17E-03	5.95E-03	2.51E-03	−6.19E-03	−.01251	−.01436	4.44E-03	1.71E-04	−6.20E-03	−5.57E-03	−6.14E-03	−.01267
$\varphi_{mg} = 45°$	R^2	.00732	.04996	.04788	.01122	.00033	.00001	.02768	.00979	.00403	.00486	.01130	.06688
($\varphi_{ms} = 90°$)	b	−1.92E-03	−3.44E-03	−4.33E-03	2.6E-03	4.14E-04	6.43E-05	−3.41E-03	−1.68E-03	−1.03E-03	−1.76E-03	2.89E-03	6.85E-03
$\varphi_{mg} = 90°$	R^2	.02513	.03156	.00030	.10604	.00200	.03632	.08244	.08929	.00460	.62937	.50003	.43073
($\varphi_{ms} = 45°$)	b	−4.54E-03	4.89E-03	−5.43E-04	5.61E-03	7.71E-04	−3.09E-03	6.83E-03	6.84E-03	1.74E-03	.01449	.01123	.01054
$\varphi_{mg} = 135°$	R^2	.04871	.78917	.36843	.13972	.21231	.45901	.10666	.14038	.02746	.07962	.04627	.07948
($\varphi_{ms} = 0°$)	b	.01099	.08601	.01686	4.39E-03	−5.86E-03	−.01140	2.1E-03	3.61E-03	1.52E-03	2.83E-03	2.51E-03	−3.97E-03
$\varphi_{sg} = 180°$													
Stand density		500 trees/hectare						1500 trees/hectare					
Tree height		10 meters			25 meters			10 meters			25 meters		
Percent cover		15			40			64			97		
Sun elevation θ_s		40°	50°	60°	40°	50°	60°	40°	50°	60°	40°	50°	60°
$\varphi_{mg} = 0°$	R^2	.01724	.84315	.79703	.27250	.20272	.57244	.13213	.00693	.03579	.42039	.03130	.49382
($\varphi_{ms} = 0°$)	b	5.02E-03	.05390	.03679	6.26E-03	−5.60E-03	−.01441	3.73E-03	5.71E-04	1.34E-03	6.75E-03	1.11E-03	−6.04E-03
$\varphi_{mg} = 45°$	R^2	.03524	.02697	.00411	.08156	.04568	.27972	.05065	.04677	.00433	.22636	.06750	.00198
($\varphi_{ms} = 45°$)	b	−3.36E-03	2.39E-03	1.02E-03	4.65E-03	−2.67E-03	−9.84E-03	3.86E-03	2.95E-03	8.79E-04	8.54E-03	4.14E-03	−5.71E-04
$\varphi_{mg} = 90°$	R^2	.10161	.00266	.00606	.00829	.07978	.05869	.28836	.09285	.07682	.00861	.07491	.08188
($\varphi_{ms} = 90°$)	b	.01390	2.10E-03	−3.18E-03	2.10E-03	−6.24E-03	−4.47E-03	.01746	7.71E-03	6.87E-03	2.19E-03	5.96E-03	6.16E-03
$\varphi_{mg} = 135°$	R^2	.01983	.00862	.00914	.05099	.03053	.31792	.7420	.02067	.00355	.39210	.05269	.02908
($\varphi_{ms} = 45°$)	b	2.69E-03	−1.56E-03	1.7E-03	3.71E-03	−2.59E-03	−.01044	4.73E-03	2.01E-03	−7.86E-04	.01294	3.4E-03	−2.11E-03

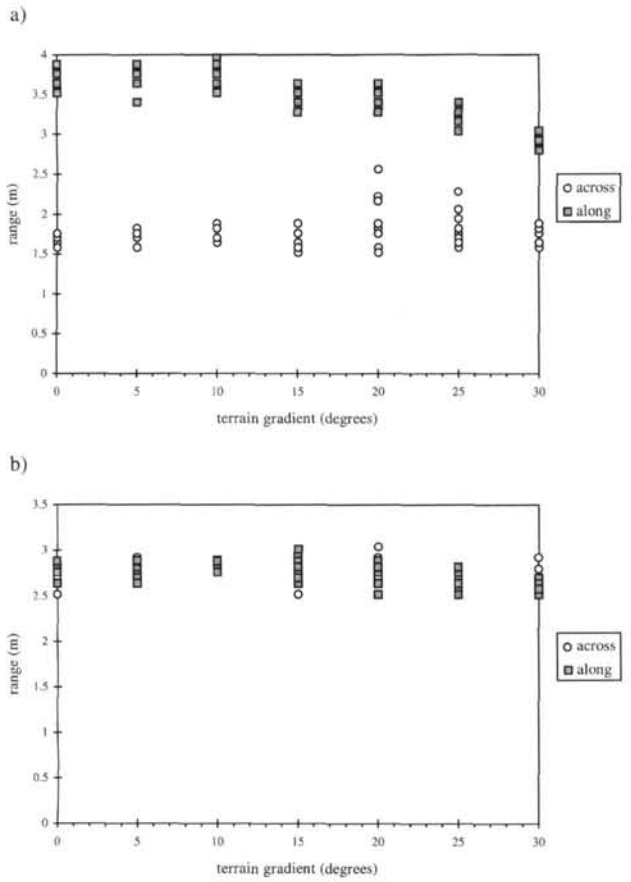

Figure 5. Comparison of the effect of terrain gradient on the range measured along (φ_{mg} = 0°) and across (φ_{mg} = 90°) the slope for softwoods (a) and hardwoods (b) at φ_{sg} = 0° and θ_s = 50° (10-m trees with a density of 500 trees/ha).

strong relationships are observed for stands having a percent cover of 15 percent (10-m trees with a 500-trees/ha density). Figure 6a shows the sharp increase of the range associated with gradient augmentation. In contrast, Figures 6b, 6c, and 6d indicate that this relationship fades when crown closure increases (40 percent, 64 percent, and 97 percent, respectively). We believe that the manner in which the tree shadows are projected determines this relationship. This matter will later be discussed in detail.

The influence of sun azimuth appears to be the dominant feature among a series of same tree size and density, while sun elevation modifies this strength in a complex fashion. When the sun faces the slope, the increase in terrain gradient brings about a drop in the semivariogram range values that actually translates into a diminution of texture coarseness (Figure 7a). However, this relationship is inverted when the sun is on the opposite side (Figure 7e). Intermediate azimuthal position shows either a transitional absence of the influence of gradient (Figure 7b) or a weaker positive influence (Figures 7c and 7d). Note that the direction in which the maximum influence is observed may change: it is generally measured in the direction parallel to the terrain gradient but may occasionally occur at oblique angles (with respect to the direction of the terrain gradient). The behavior associated with varying the sun elevation from 40 to 60 degrees is itself variable. The strongest relations of a series with constant forest and azimuth conditions are observed for either the low, medium, or high sun elevation, depending apparently on the sun azimuth.

One noticeable constant is the almost perfect absence of a relationship between the slope and texture coarseness when the semivariogram is measured perpendicularly to the gradient. This phenomenon is observable in every situation. It is evident in Figures 3 and 7e where ranges measured in the direction parallel to the gradient nearly double while the ranges measured in the other direction remain constant. This stability would undoubtedly help in an eventual correction method.

Discussion

Results generally show that a strong influence of terrain gradient is observable in cases where percent cover is low. This leads us to believe that topographic effects essentially depend on the projection of shadows on the ground. Figure 8 shows the appearance of trees and shadows for a very simple situation (trees are aligned) and for the extreme gradients used in this study (0 and 30 degrees). We see in Figures 8a and 8b that, when trees are separated by a relatively long distance, the influence of gradient is very apparent: shadows become shorter (if the sun is facing the slope), thus affecting the structure of the alternance of light and dark patterns. However, when trees are close to each other, as in Figures 8c and 8d, the effect of gradient is very subtle, for the projected shadows fall essentially on other trees.

The variation of the topography-texture relation observed for different sun azimuths is due to the changes in shadow length. When the sun is facing the slope, the increase of gradient causes a decrease in shadow length that determines a drop in texture coarseness and, thus, in the range of the semivariogram measured in the direction of the gradient and the incident light. Inversely, when the sun is positioned on the opposite side, the increase in gradient is followed by an elongation of the shadows, and a range increase. The nearly complete absence of variation of the ranges measured in the direction perpendicular to the gradient is explained by the fact that the inter-tree height relations are not affected by gradient augmentation in that particular direction.

We have demonstrated in this study that the slope of the terrain underlying the canopy can have, at least in some instances, a very strong effect on the ranges and that estimates of the forest structure can thus be affected by topography. Correcting the effect of gradient, in real situations, so that reliable estimates of stand parameters can be obtained through image processing appears feasible for the following reasons:

- sun position at the moment of image acquisition and the gradient and azimuth of gradient can be obtained through tables and from a digital elevation model;
- cases where a correction may be needed — stands with low percent cover — can be identified by their strong range anisotropy and/or by the uncorrected estimates that clearly indicate the presence of a sparse stand (using Equation 3, for example), even if error affect these estimates;
- the mathematical relation between gradient and the range of the semivariogram, being in most cases linear, can be easily modeled;
- the shape of the trees, on which may depend the exact calibration of the correction model, can be derived by classical means through a classification of softwood and hardwood; and
- there is always a known direction of reference in which the range is invariable.

In spite of the relatively high number of different combinations of stand characteristics and sun-terrain configurations analyzed, there remains a certain number of situations, and potentially important factors, not considered in this study that would need special attention to reach a more thorough understanding of topography-texture relationships. First, the

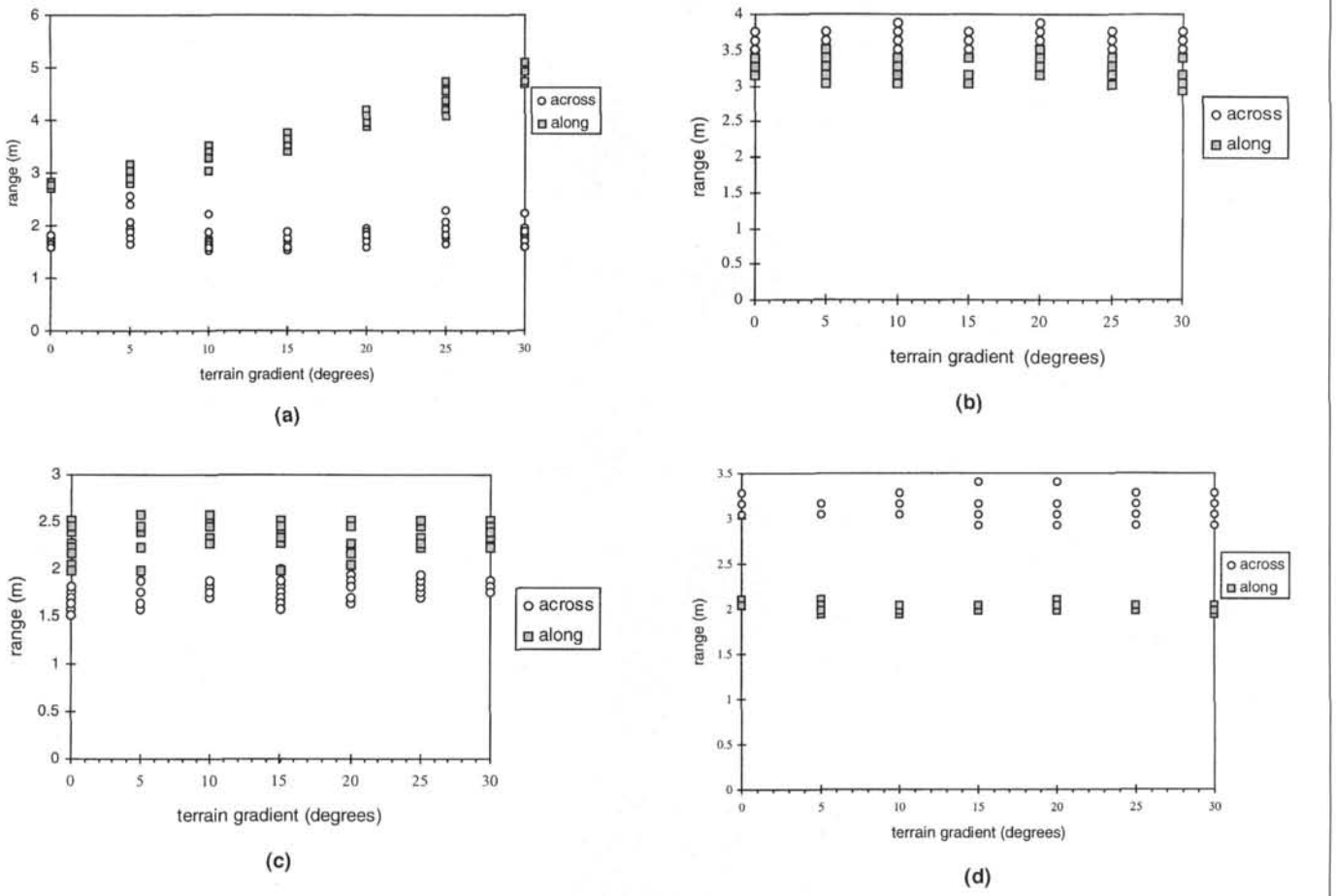

Figure 6. Effect of terrain gradient on the range for softwood stands having a percent cover of 15 percent (a), 40 percent (b), 64 percent (c), and 97 percent (d).

presence of concavities, convexities, or sharp drops in the profile of the terrain, for example, could have a particular effect on local texture coarseness because of the specific three-dimensional configuration of the canopy associated with these situations. Second, the very particular cases of crests or hill tops should also be studied. However, it appears reasonable to assume that these circumstances have in most cases only a very local impact on texture and do not bring important limitations to our conclusions. Indeed, mild curvatures can be modeled by a series of flat grading segments, for which we can apply the knowledge developed in this study. Because high terrain curvatures can only be local, an eventual gradient-corrected forest structure mapping method could skip these curved areas and interpolate values to fill the resulting gaps. Third, image texture could be influenced by understory structures in the case of open canopies, thus complicating the effect of topography. We believe, however, that because understory structures are composed of smaller trees or bushes having a diameter close to the one-meter resolution used in this study, their influence on the semivariogram would be felt at the level of the nugget effect, i.e., the magnitude of the semivariance corresponding to the first h increment, and would not for this reason affect the ranges. Finally, we must consider the fact that results were obtained using computer-simulated images generated using models for tree shape, stand structure, and light propagation. While these images were shown to recreate realistic textures, some precaution must accompany the use of the results because items such as forest gaps, complex vertical stratification, specific spatial tree distributions, or spectral band differences are not considered in our stand modeling approach, which is however one of the most efficient means to reach any statistically significant results on the issue of topographic effects.

Conclusions

The influence of terrain gradient on the texture measured by the semivariogram on high-resolution computer-simulated images of forest stands was evaluated by varying the gradient of forest-covered slopes from 0 to 30 degrees for different forest types and illumination geometry recreated by computer modeling. For hardwoods or softwoods, this influence was found to be significant only in a few situations: it was indeed most noticeable for opened forest canopies, especially when the sun was in line with the azimuth of the gradient (facing or at the back of the slope). However, even in extreme cases, the estimated values of tree size and density were not dramatically altered. It also appeared that there is, for every stand-illumination combination, a direction in which the texture measure is not affected. Despite limitations in the modeling procedure, we conclude that topographic effects on the texture of one-meter-resolution images are minor and theoretically correctable, and that they don't constitute a major obstacle to precise mapping of the structure of the forest by automated processing of high resolution images.

Acknowledgments

Funding for this project was provided by the Natural Sciences and Engineering Research Council of Canada (grant #

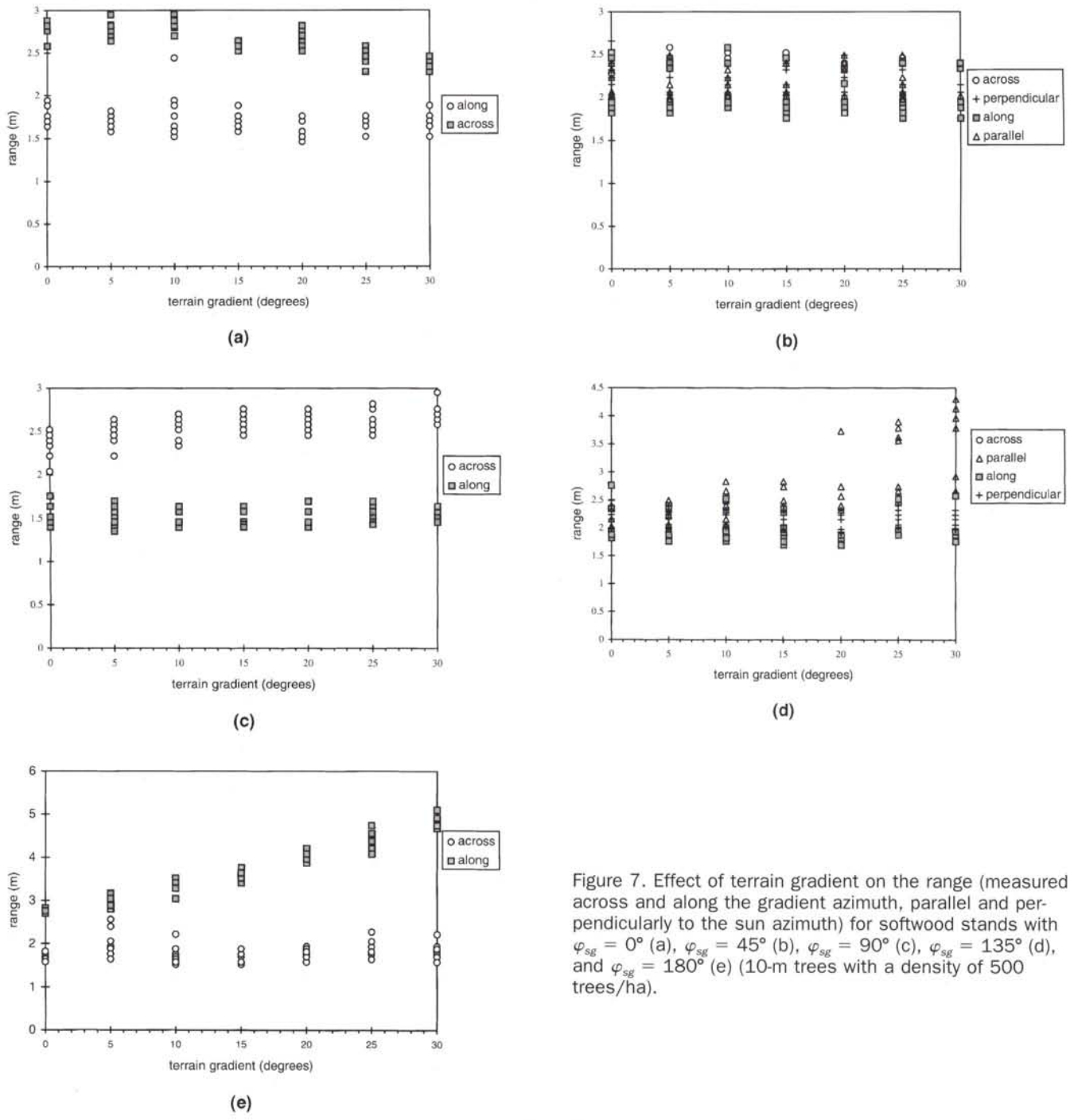

Figure 7. Effect of terrain gradient on the range (measured across and along the gradient azimuth, parallel and perpendicularly to the sun azimuth) for softwood stands with $\varphi_{sg} = 0°$ (a), $\varphi_{sg} = 45°$ (b), $\varphi_{sg} = 90°$ (c), $\varphi_{sg} = 135°$ (d), and $\varphi_{sg} = 180°$ (e) (10-m trees with a density of 500 trees/ha).

DGP0184009). We wish to thank Mr. Martin Couture for his help in preparing the data compilations, and the Canada Centre for Remote Sensing for permission to use the MEIS II images. Our appreciation also goes to the Petawawa National Forest Institute staff, particularly to Dr. Don Leckie, for providing access to useful ground data, and to Dr. François Gougeon, for his assistance in transferring the MEIS II images.

References

Atkinson, P.M., and F.M. Danson, 1988. Spatial resolution for remote sensing of forest plantations, *Proceedings of IGARSS '88 Symposium*, Edinburgh, Scotland, 13-16 September 1988, ESA SP-284, IEEE 88CH2497-6, pp. 221–223.

Avery, E.A., and H.E. Burkhart, 1983. *Forest Measurements*, McGraw-Hill, New York, 331 p.

Barker Schaaf, C., X. Li, and A.H. Strahler, 1994. Topographic effects on bidirectional and hemispherical reflectances calculated with a geometric-optical canopy model, *IEEE Transactions on Geosciences and Remote Sensing*, 32(6):1186–1193.

Cohen, W.B., T.A. Spies, and G.A. Bradshaw, 1990. Semivariograms of digital imagery for analysis of conifer canopy structure, *Remote Sensing of Environment*, 34(3):167–178.

Dikshit, O., 1996. Textural classification for ecological research using

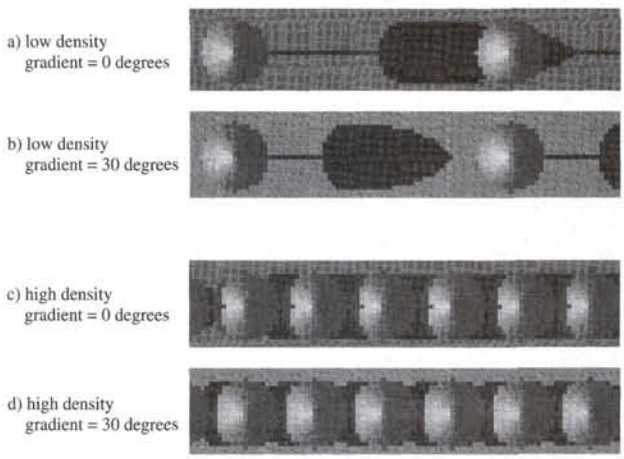

Figure 8. Influence of density-dependent inter-tree distance on the shadow elongation of 20-m softwood trees (resolution was exceptionally set at 25 cm).

ATM images, *International Journal of Remote Sensing*, 17(5): 887–915.

Dikshit, O., and D.P. Roy, 1992. An empirical investigation of image resampling effects upon the spectral and textural supervised classification of a high spatial resolution multispectral image, *Photogrammetric Engineering & Remote Sensing*, 62(9):1085–1092.

Dreyer, P., 1993. Classification of land cover using optimized neural nets on SPOT data, *Photogrammetric Engineering & Remote Sensing*, 59(5):617–621.

Ekstrand, S., 1996. Landsat TM-based forest damage assessment: Correction for topographic effect, *Photogrammetric Engineering & Remote Sensing*, 62(2):151–61.

Franklin, S.E., W. Bowers, J. Hudack, and G. McDermid, 1992. Estimating structural damage in balsam fir stands using semivariance, *Proceedings of the 15th Canadian Symposium on Remote Sensing*, Vancouver, pp. 96–99.

Gougeon, F.A., and A.K.C. Wong, 1987. Towards a knowledge-based spectral and textural signature recognition, *Proceedings of the 11th Canadian Symposium on Remote Sensing*, Waterloo, Ontario, pp. 565–578.

Hafley, W.I., and H.T. Schreuder, 1977. Statistical distributions for fitting diameter and height data in even aged stands, *Canadian Journal of Forest Research*, 7:481–489.

Hamilton, S., 1996. High resolution data presents new possibilities, *Earth Observation Magazine*, 5(11):37–38.

Haralick, R.M., 1979. Statistical and structural approaches to texture, *Proceedings of the IEEE*, 67(5):786–804.

———, 1986. Statistical image texture analysis, *Handbook of Pattern Recognition and Image Processing* (X.X. Young and X.X. Fu, editors), Academic Press, New York, pp. 247–279.

Hawkins, J.K., 1970. Textural properties for pattern recognition, *Picture Processing and Psychopictorics* (B.S. Lipkin and A. Rosenfeld, editors), Academic Press, New York, pp. 347–371.

Howard, J.A., 1970. *Aerial Photo-Ecology*, American Elsevier Publishing Company, New York, 325 p.

Kashyap, R.L., 1986. Image models, *Handbook of Pattern Recognition and Image Processing* (X.X. Young and X.X. Fu, editors), Academic Press, New York, pp. 282–310.

Koop, H., 1989. *Forest Dynamics*, Springer-Verlag, Berlin, 229 p.

Küchler, A.W., 1967. *Vegetation Mapping*, The Ronald Press Company, New York, 472 p.

Levine, M.D., 1985. *Vision in Man and Machine*, McGraw-Hill, New York, 574 p.

Li, X., and A.H. Strahler, 1985. Geometric-optical modeling of a conifer forest canopy, *IEEE Transactions on Geoscience and Remote Sensing*, 23(5):705–720.

Marceau, D.J., X.X. Howarth, P.J. Dubois, and D.J. Gratton, 1990. Evaluation of the gray level occurrence matrix for land cover classification using SPOT imagery, *IEEE Transactions on Geoscience and Remote Sensing*, 28(4), 513–519.

Matheron, G., 1970. *La théories des variables régionalisées et ses applications*, Les Cahiers du Centre de Morphologie Mathématique de Fontainebleau, # 5, Fontainebleau, France, 212 p.

McKelvey, K.S., 1987. A geometric model of sunlight penetration for slash pine in northern Florida, *Proceedings of the IUFRO Conference*, pp. 322–331.

Miner, C.L., N.R. Walters, and M. Belli, 1988. *A Guide to the TWIGS Program for the North Central United States*, General Technical Report NC-125, North Central Experimental Station, USDA, Forest Service, St-Paul, Minnesota, 105 p.

Rowland, J.D., and R.D. Moore, 1992. Modelling solar irradiance on sloping surfaces under leafless deciduous forests, *Agricultural and Forest Meteorology*, 60:111–132.

Ryherd, S., and C. Woodcock, 1996. Combining spectral and texture data in the segmentation of remotely sensed images, *Photogrammetric Engineering & Remote Sensing*, 62(2):181–194.

Spurr, S.H., 1960. *Photogrammetry and Photo-Interpretation: With a Section on Application to Forestry, Second Edition*, The Ronald Press Company, New York, 472 p.

Stiell, W.M., 1962. *Crown Structure in Red Pine Plantations*, Technical Note No. 122, Forest Research Branch, Canadian Department of Forestry, Ottawa, 12 p.

St-Onge, B.A., and F. Cavayas, 1995. Estimating forest stand structure from high resolution imagery using the directional variogram, *International Journal of Remote Sensing*, 16(11):1999–2021.

———, 1997. Automated forest structure mapping from high resolution imagery based on directional semivariogram estimates, *Remote Sensing of Environment*, 61:82–95.

St-Onge, B.A., F. Cavayas, and P.M. Teillet, 1991. Étude de la signature spatiale des couverts forestiers par modélisation géométrique-optique, *Proceedings of the 5th International Symposium on Physical Measures and Signatures in Remote Sensing*, Courchevel, France, 14–18 January, ESA SP-319, pp. 671–674.

Stromberg, W.D., and T.G. Farr, 1986. A Fourier based textural feature extraction procedure, *IEEE Transactions on Geoscience and Remote Sensing*, 24(5):722–731.

Tamura, S., S. Mori, and T. Yamawaki, 1978. Textural features corresponding to visual perception, *IEEE Transactions on System, Man and Cybernetics*, 8:460–473.

Teillet, P.M, D.G. Goodenough, and B. Guindon, 1981. Digital analysis of spatial and spectral features from airborne MSS of a forested region, *Proceedings of the 15th Symposium on Remote Sensing of the Environment*, pp. 883–903.

Till, S.M., R.A. Neville, D.G. Leckie, and W.M. Strome, 1987. Advanced airborne electro-optical imager, *Proceedings of the 21st International Symposium on Remote Sensing of Environment*, Ann Arbor, Michigan, 26–30 October, pp. 41–47.

Unser, M., 1995. Texture classification and segmentation using wavelet frames, *IEEE Transactions on Image Processing*, 4(11): 1549–1560.

Vlcek, J., D.Jayasinghe, D.King, X.Yuang, and F. Cadeau, 1987. Spectral and spatial classification of land-cover types in multispectral aerial video imagery, *Proceedings of the 11th Canadian Symposium on Remote Sensing*, Waterloo, Ontario, 22–25 June, pp. 99–107.

Wang, L., and D.C. He, 1990. A new statistical approach for texture analysis, *Photogrammetric Engineering & Remote Sensing*, 56(1): 61–66.

Woodcock, C.E., A.H. Strahler, and D.L.B. Jupp, 1988. The use of variograms in remote sensing: II - Real digital images, *Remote Sensing of Environment*, 25(4):349–379.

(Received 10 February 1997; revised and accepted 29 April 1998; revised 08 September 1998)